Cellular Signalling 61 (2019) 39–47

Contents lists available at ScienceDirect

Cellular Signalling

journal homepage: www.elsevier.com/locate/cellsig

Keratinocyte growth factor (KGF) induces podosome formation via integrin-Erk1/2 signaling in human immortalized oral epithelial cells

Guoliang Sa[a,b], Zhikang Liu[a], Jiangang Ren[a,b], Qilong Wan[a,b], Xuepeng Xiong[a,b], Zili Yu[a,b], Heng Chen[a], Yifang Zhao[a,b], Sangang He[a,b,*]

[a] The State Key Laboratory Breeding Base of Basic Science of Stomatology (Hubei-MOST) & Key Laboratory of Oral Biomedicine Ministry of Education, School & Hospital of Stomatology, Wuhan University, Wuhan, China
[b] Department of Oral Maxillofacial Surgery, School & Hospital of Stomatology, Wuhan University, Wuhan, China

ARTICLE INFO

Keywords:
Mouth mucosa
Cell-matrix junction
Matrix metalloproteinase
Podosomes
Cortactin
Actin

ABSTRACT

Recent study established the role of integrins in keratinocyte growth factor (KGF)-induced oral epithelial adhesion and rete peg elongation. However, how extracellular matrix (ECM) remodeling cooperates with the increased epithelial adhesion during rete peg elongation has yet to be determined. Podosomes are cell-matrix contact structures that combine several abilities, including adhesion and matrix degradation. In the present study, we identified podosome formation at the ventral side of human immortalized oral epithelial cells (HIOECs) upon KGF treatment. Moreover, podosomal components including integrin α6 , β4 , α3 , β1 and MMP14 colocalized with the F-actin-cortactin complex and matrix degradation assays demonstrated the ability of the F-actin-cortactin complex to degrade matrix. Inhibition both of integrin subunits β4 and β1 with specific blocking antibodies and inhibition of Erk1/2 abrogated the KGF-induced podosome formation. Notably, knockdown of integrin subunits β4 and β1 with specific small interfering RNA (siRNA) downregulated the phosphorylation levels of Erk1/2. In contrast, inhibition of both Erk1/2 could upregulate the expression of integrin subunits β4 and β1. These results demonstrate that KGF induces podosome formation via integrin-Erk1/2 signaling in HIOECs, suggesting a novel mechanism by which integrins enhance oral epithelial adhesion and rete peg elongation.

1. Introduction

Oral mucosal rete pegs are epithelial protrusions toward the lamina propria formed by epithelial cell proliferation and migration upon various factors such as mechanical stimuli [1,2]. An increasing number of studies demonstrate that rete pegs contribute to epithelial adhesion because they can enlarge the contact area between the oral epithelium and lamina propria [3]. However, the extracellular matrices (ECM) underlying the basement membrane dynamically remodel during the progress of rete peg elongation, which may compromise epithelial adhesion. Consequently, how ECM remodeling cooperates with increased epithelial adhesion during rete peg elongation has yet to be determined.

Podosomes are dynamic cell-matrix contact structures that combine several key abilities, including adhesion and matrix degradation, via their expression of integrins and matrix metalloproteases (MMPs) [4,5]. Although the first description of podosomes was in Rous sarcoma virus-transformed fibroblasts as aberrant adhesion structures and subsequently in several cell types of mesenchymal origin including osteoclasts and macrophages, they are not unique to cells of mesenchymal origin [5]. Endothelial cells can form podosomes quickly after short-term treatment with TGFβ, TNF-α, VEGF, and phorbol ester [6,7]. Moreover, these podosomes could organize into rosette structures that were the precursors of new vascular branching points [6,8]. Phorbol esters can also activate human bronchial epithelial cells and have been implicated in not only podosome assembly but also recruitment of MMPs to podosomes for matrix degradation [9]. Most importantly, the skin-derived keratinocyte cell line HaCat also displayed podosome-like structures [10]. Based on these studies, we hypothesize that oral epithelial cells have the possibility to form podosomes upon growth factor treatment.

Abbreviations: HIOECs, human immortalized oral epithelial cells; KGF, keratinocyte growth factor; KGFR, keratinocyte growth factor; MAPK, mitogen-activated protein kinases; Jak-Stat, Janus kinase-signal transducers and activators of transcription; ECM, extracellular matrix; MMP, matrix metalloproteases; DAPI, 4′,6-Diamidino-2-Phenylindole, Dihydrochloride; siRNA, small interfering RNA; KSFM, keratinocyte serum-free medium; WASP, Wiskott-Aldrich syndrome protein.

* Corresponding author at: School & Hospital of Stomatology, Wuhan University, Wuhan 430079, China.
E-mail address: sangang@whu.edu.cn (S. He).

https://doi.org/10.1016/j.cellsig.2019.05.007
Reçu le 10 janvier 2019; Reçu en forme révisée le 8 mai 2019; accepté le 9 mai 2019
Available online 10 May 2019
0898-6568/ © 2019 Published by Elsevier Inc.

Our previous study demonstrated that KGF simultaneously enhanced oral rete peg elongation and epithelial adhesion, suggesting the possibility that KGF may induce podosomes formation [11]. In this study, we identified the formation of podosome structures by colocalization among F-actin, cortactin, vinculin, and Wiskott-Aldrich syndrome protein (WASP) in HIOECs 24 h after KGF treatment by confocal microscopy. Moreover, we analyzed the colocalization of podosomal components including integrin α6 , β4 , α3 , β1 and MMP14 with F-actin-cortactin and the ability to degrade matrix. Additionally, we explored the related signaling molecules that regulate podosomes formation in HIOECs after KGF treatment. Because the mitogen-activated protein kinases (MAPK) pathway, the Akt pathway, and the Janus kinase-signal transducers and activators of transcription (Jak-Stat) pathway are three main signaling pathways that mediate the effects of growth factors and cytokines on epithelial cells [12–14], the phosphorylation of Erk1/2, p38, Jnk, Akt, Jak2, and Stat3 were detected by Western blot.

2. Materials and methods

2.1. Antibodies and reagents

Antibodies used for functional blockade are shown in Table 1. Antibodies used for Western blot are shown in Table 2. HYD-1 (a D-amino acid-containing peptide with amino acid sequence: Lys-Ile-Lys-Met-Val-Ile-Ser-Trp-Lys-Gly) was purchased from Wuhan Bioyeargene Biotechnology Co., Ltd. (Wuhan, Hubei, China). MMP14 was purchased from abcam (ab3644). WASP was purchased from HuaBio (EM1706–58, Hangzhou China). Vinculin was purchased from merck-millipore (MAB3574). A FITC Phalloidin and an Acti-stain™ 670 phalloidin were obtained from AAT Bioquest Inc. An Erk1/2 inhibitor U0126, and Akt inhibitor Ly294002 and MK2206 were obtained from Selleck chemicals (Selleck, USA). The β4 and β1 siRNA kitswere obtained from Ribobio (Guangzhou, China).

2.2. Cell culture and treatment

The HIOEC line was established by the Shanghai Key Laboratory of Stomatology, which was obtained from normal oral mucosa immortalized with HPV16 E6/E7 gene transfection [15]. HIOEC line was authenticated by VivaCell Bioscience (Shanghai, China) using short tandem repeat (STR) markers (Report No.:VC20190428003). Detection of mycoplasma contaminations showed that HIOEC cell was not contaminated. HIOECs were cultured in keratinocyte serum-free medium (KSFM; Gibco) in a humidified atmosphere containing 5% CO_2 at 37 °C. When the cells were grown to 70%–80% confluence, they were passaged using 0.25% trypsin (Invitrogen, CA, USA) solution according to standard protocols. For confocal immunofluoresence microscopy, cells were seeded in the tissue culture treated 24-well plates (NEST, Wuxi, China) (1.4×10^5 cells per well). Cells grown on microscope coverslips were rinsed in PBS and then fixed in 4% paraformaldehyde at 37 °C for 5 min. The cells were incubated with the primary antibody over-night in a humidified chamber at 4 °C. After washing, the cells were incubated with the secondary antibody (Alexa-Flour 488 goat anti-rabbit IgG; Life Technologies) in a humidified chamber for 1 h at room temperature. Finally, the cells were mounted with Mounting Medium supplemented with 4′, 6-Diamidino-2-Phenylindole, Dihydrochloride (DAPI) (ZLI-9557, ZSGB-BIO, Beijing). Olympus microscope system FV1000 (Olympus, Tokyo, Japan) was employed. Images acquisition was performed using Olympus FluoView™ FV10-ASW 4.2 Wiewer (Olympus, Tokyo, Japan) with a 100× oil-immersion objective (UPLSAPO100XS; NA, 1.40). 405 (HV, 474; Gain, 2; offset 6%), 488 (HV, 596; Gain, 2; offset 7%), and 559 (HV, 628; Gain, 2; offset 6%) nm emission wavelength lasers were used. For real-time PCR, Western blot, and transfection assay, the cells were seeded in 6-well plates (8×10^5 cells per well). Cells were given the indicated treatment.

Table 1
Antibodies used for function blocking assay.

Antibody	Host	Source	Dilution
Integrin α6 (G0H3)	Rat	Biolegend (313613)	1:20
Integrin β4 (3E1)	Mouse	Millipore (MAB1964)	1:20
Integrin α3 (P1B5)	Rabbit	Millipore (MAB1952)	1:20
Integrin β1 (12G10)	Mouse	Abcam (ab30394)	1:20

Table 2
Antibodies used for Western blot.

Antibody	Host	Source	Dilution
Akt (pan)	Rabbit	CST (#4691)	1:1000
Integrin α6	Rabbit	Abcam (ab133386)	1:1000
Integrin β4	Rabbit	Abcam (ab182120)	1:1000
Integrin α3	Rabbit	Novus (NBP1–19724)	1:1000
Integrin β1	Rabbit	Novus (NB110–510)	1:1000
Erk1/2	Rabbit	CST (#9102)	1:1000
Jak2	Rabbit	CST (#3230)	1:1000
Jnk	Rabbit	CST (#9252)	1:2000
P38	Rabbit	CST (#9212)	1:1000
Phospho-Akt (Ser473)	Rabbit	CST (#4060)	1:1000
Phosphor-P38(Thr180/Tyr182)	Rabbit	CST (#9211)	1:1000
Phosphor-Erk1/2 (Thr202/Try204)	Rabbit	CST (#8544)	1:1000
Phosphor-Jak2 (Tyr1007)	Rabbit	CST (#4406)	1:1000
Phosphor-Jnk (Thr183/Tyr185)	Rabbit	CST (#9251)	1:1000
Phosphor-Stat3 (Tyr705)	Rabbit	CST (#9135)	1:1000
Stat3	Mouse	CST (#9139)	1:1000

2.3. Integrin function-blocking assays

Cells were preincubated with HYD-1 or functional blocking antibodies against α6 (GoH3), α3 (clone P1B5), β4 (clone 3E1), and β1 (clone 12G10) integrin subunits or mouse control IgG at a final concentration at 20 μg/ml at room temperature for 10 min before KGF treatment.

2.4. Matrix degradation assay

Briefly, 150 μl (1 mg/ml) Alexa Fluor 594-labeled Matrigel was dropped onto coverslips for 1 h at room temperature, forming about 1.0 mm coating onto the bottom. Then, HIOECs were seeded onto Matrigel-coated coverslips in 24-well plates and grown for 24 h. An Alexa Fluor® 594 Protein Labeling Kit (Thermo fisher scientific, A10239) was used to label Matrigel for the ECM degradation assays. The cells were grown on glass coverslips and given the indicated treatment for 24 h. Then, cells were washed with PBS, fixed in 4% paraformaldehyde at room temperature for 5 min, and blocked with 10% nonimmune goat serum for 1 h at room temperature. After that, cells were incubated with primary antibody to cortactin at a dilution of 1:100 overnight at 4 °C, followed by incubation with Alexa Fluor® 488-conjugated secondary antibody (1:200) and Acti-stain™ 670 phalloidin for 1 h at room temperature. Confocal fluorescent images were acquired with an Olympus inverted laser scanning fluorescence microscope equipped with acquisition software (FV1000, Tokyo, Japan) and a NA 1.4 oil immersion objective. Triple imaging for Acti-stain™ 670 phalloidin, Alexa-Fluor-488-cortactin, and Alexa-Fluor-594-labeled Matrigel was performed using selective laser excitation at 405, 488 and 559 nm, respectively. Each channel was imaged sequentially using the multitrack recording module before merging. Cells showing podosomes were quantified by scoring at least 300 cells for each coverslip. Degradation index was computed using the ImageJ Analyze Particles function by taking the mask of punctiform blackening within the fluorescently labeled gelatin due to podosomal collagenolytic activity. 10 fields (for degradation) were analyzed per experimental group.

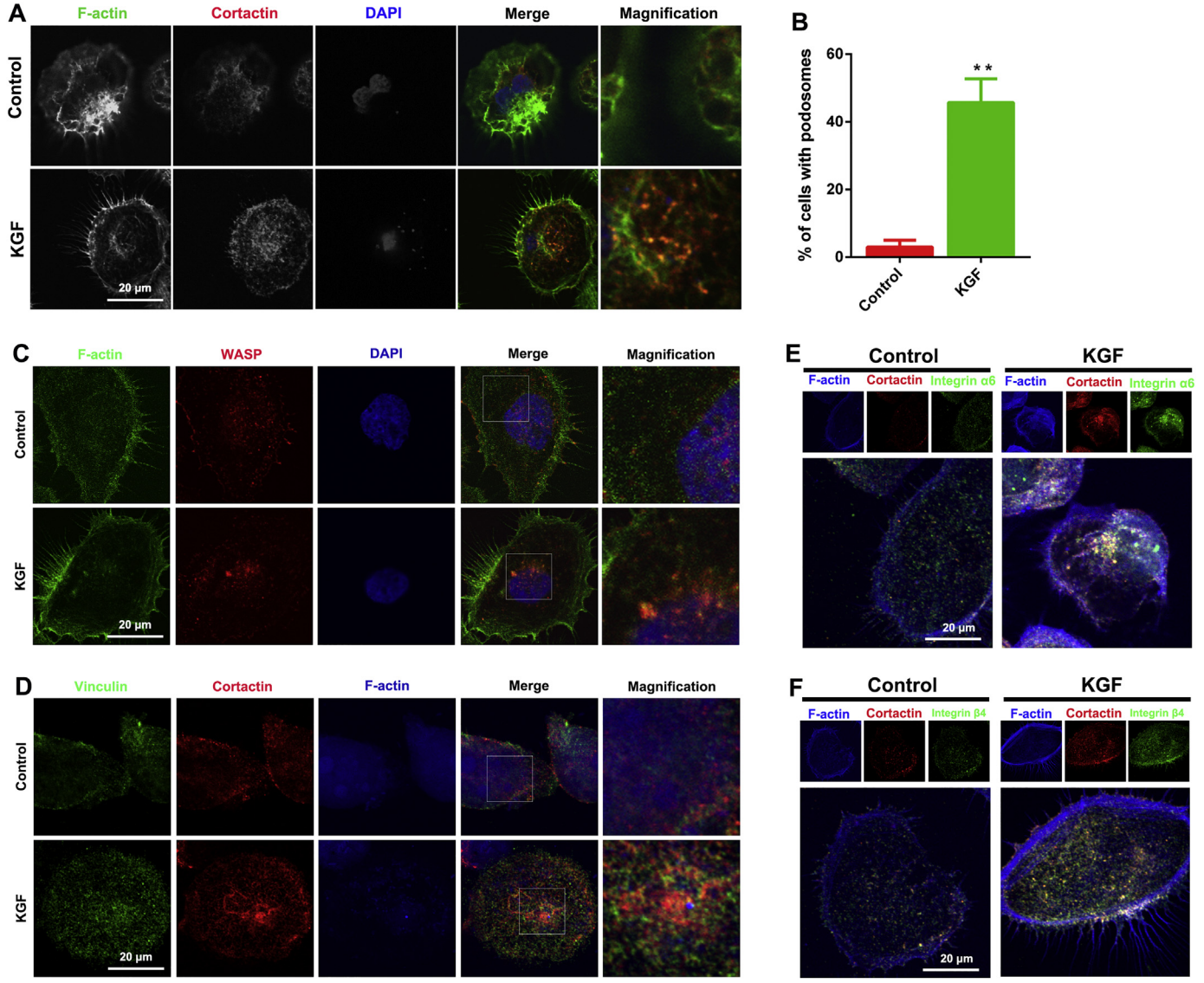

Fig. 1. KGF induces the assembly of podosome structures in HIOECs. (A and B) 24 h after KGF treatment, the ratio of cells containing F-actin-cortactin complexes in the KGF group was significantly elevated compared to the control group. $n = 3$ independent experiments in which 100 cells per experimental point were analyzed. Data are expressed as the mean ± SD. $^{**}P < 0.01$. (C and D) Colocolization of WASP with F-actin and colocolization of vinculin with cortactin was invisible in HIOECs of control group. WASP was colocalized with F-actin in the center of podosome, whereas vinculin was surround F-actin, and localized in the ring of pososome in KGF group. (E and F) 24 h after KGF treatment, the colocalization among integrin subunit α6, β4 and F-actin-cortactin complexes. Control: HIOECs cultured in normal KSFM; KGF: HIOECs cultured in normal KSFM supplemented with KGF at a concentration of 10 ng/mL.

Integrated density was used as readout.

2.5. Small interfering RNA (siRNA) transfection

HIOECs at a density of 40% confluence were serum-deprived for 24 h for transfection. Interference of integrin subunits β4 and β1 expression was performed by transfecting Lipofectamine 2000 with integrin-targeted siRNA and the universal negative control siRNA according to the manufacturer's protocol. The sequences of the siRNAs against Integrin β4 was (GGAAAGAGCTGCAGGTGAA) and siRNAs against Integrin β1 (GCGAGTGTGATAATTTCAA). Knockdown efficacy was confirmed by Western blot and real-time RT PCR 48 h after transfection.

2.6. Western blot and analysis

Proteins were collected, and the supernatant protein concentration was estimated using the BCA assay (Pierce, Rockford, IL, USA). Subsequently, 20 μg of protein was separated on 10% SDS-polyacrylamide gels and transferred onto PVDF membranes (Roche Applied Science). The blots were blocked overnight with 5% non-fat dry milk and probed with primary antibodies at 1:1000 dilutions. The immunoblots were detected with HRP-conjugated secondary antibody (Pierce, Rockford, IL, USA) using a chemiluminescence kit (Pierce, Rockford, IL, USA). The semiquantitative analysis of Western blots was carried ImageJ software. Specifically, it could be divided into the following steps. 1) Open the image in Image J. 2) Convert the image into grayscale picture. 3) Subtract the background. 4) Set integrated density. 5) Set scales. 6) Invert the image into bright band. 7) Acquire the integrated gray values of the respective bands by freehand selection. The expression levels of indicated proteins were revealed by the calculating ratio of a special molecule to GAPDH, α-tubulin or β-Actin.

2.7. Real-time PCR

Total RNA was isolated from 10^6 HIOECs using TRIzol reagent

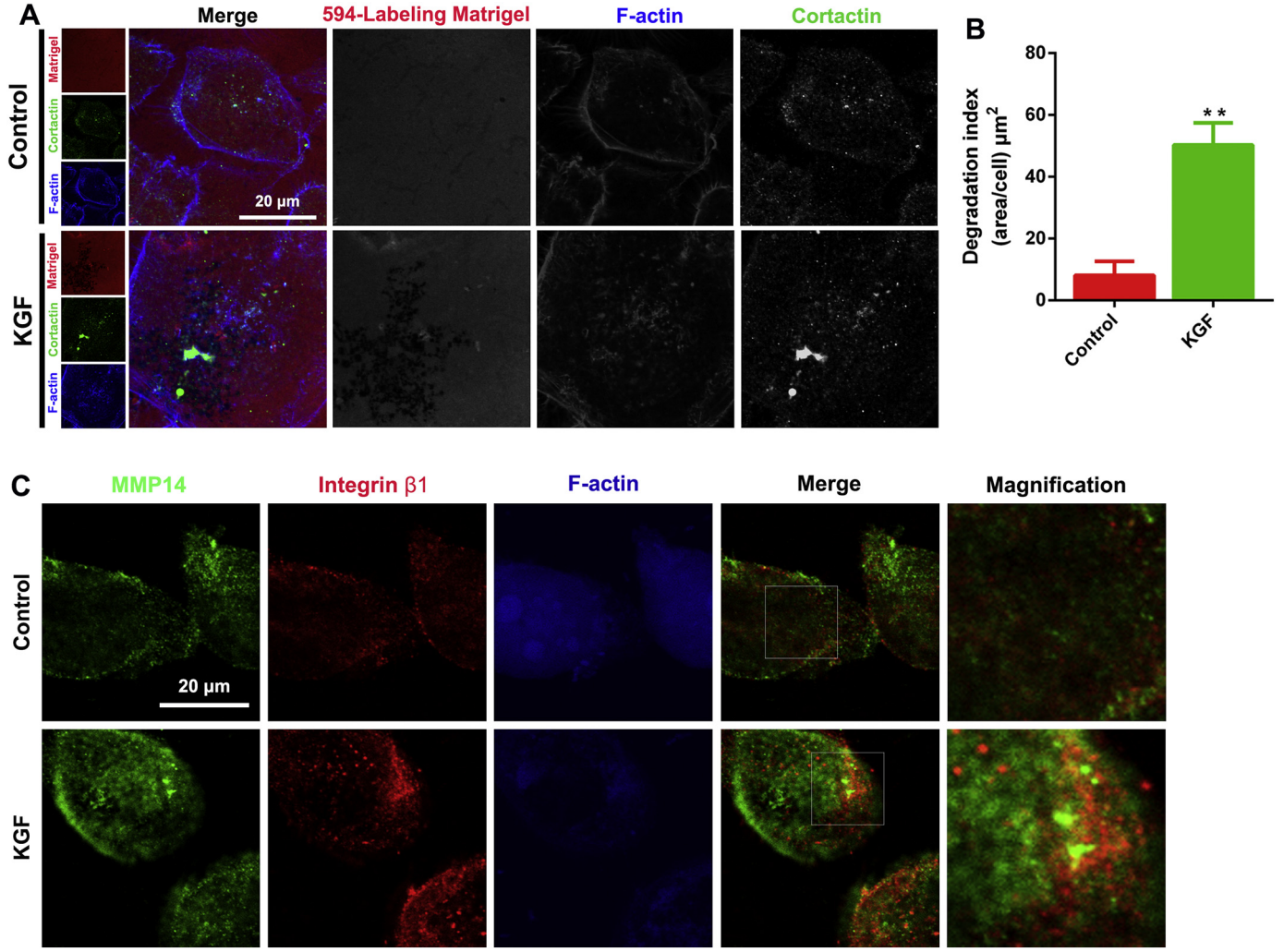

Fig. 2. The matrix-degradation ability of podosomes in HIOECs. (A and B) The Matrigel degradation ability of HIOECs in the KGF group was much higher than that of the control group. Calculation of degradation areas on fluorescence-labeled Matrigel was performed for at least 10 fields (×10 objective lens) for each coverslip. The areas of degradation were measured by the Analyze Particles function of ImageJ software. The loss of matrix-associated fluorescence (total degraded areas) is expressed as the intensity of matrix degradation. Then the total degradation area (presented in μm^2) was normalized for the degradation index (area (μm^2)/cell). $n = 3$ independent experiments in which 10 cells per experimental point were analyzed. Data are expressed as the mean ± SD. $^{**}P < 0.01$. (C) Colocolization of among MMP14, integrin β1 and F-actin was invisible in HIOECs of control group, whereas the colocolization among MMP14, integrin β1 and F-actin was easily detected in HIOECs of the KGF group.

(Gibco BRL Life Technologies, Gaithersburg, MD, USA) following the manufacturer's instructions. First-strand cDNA was synthesized from 1 μg total RNA in a final volume of 20 μl using a First Strand cDNA Synthesis Kit (Takara, Dalian, China). After reverse transcription, amplification was carried out by PCR using Taq DNA polymerase and a dNTP Set (Fermentas, Thermo Fisher Scientific, Glen Burnie, MD, USA). The following PCR conditions were used for all PCRs: 94 °C 10 min, 60 °C 90 s, and 72 °C 120 s. The primer nucleotide sequences for PCR are presented below. Integrin β4 (Forward, 5′-GCAGCTTCCAAATCAC AGAGG-3′, Reverse, 5′-CCAGATCATCGGACATGGAGTT-3′). Integrin β1 (Forward, 5′-CCTACTTCTGCACGATGTGATG-3′; Reverse, 5′-CCTTTGC TACGGTTGGTTACATT-3′). Reference gene GAPDH (Forward, 5′-CAA CCGTGAAAAGATGACCC-3′; Reverse, 5′-GTCTCCGGAGTCCATCA CAA-3′). Three separate experiments were performed on different cultures, and each sample was assayed in triplicate. A mean value was used to determine the mRNA levels using the comparative Cq method with the formula $2^{-\Delta\Delta Cq}$ ($2^{-\Delta\Delta Ct}$).

2.8. Statistical analysis

All data were analyzed with Student's *t*-test at a significance level of $P < .05$ in GraphPad Prism 6.0 (GraphPad Software, Inc.). The results are expressed as mean ± SD for 3 independent experiments.

3. Results

3.1. KGF induces the assembly of podosome structures in HIOECs

To verify our hypothesis that KGF can promote the formation of podosomes, we firstly detected the colocalization of F-actin and cortactin 24 h after KGF treatment by confocal microscopy. The results showed that colocalization of F-actin and cortactin was almost invisible in HIOECs of control groups (Fig. 1A), whereas 40%–50% of HIOECs showed colocalization of F-actin and cortactin 24 h after KGF treatment (Fig. 1B). These podosome-like structures presented as dot-like structures with a diameter approximately 0.4 μm (Fig. 1A, magnification). Podosomes characteristically contain WASP, cortactin, Arp2/3, and F-actin in the center, which is surrounded by a ring of integrin and

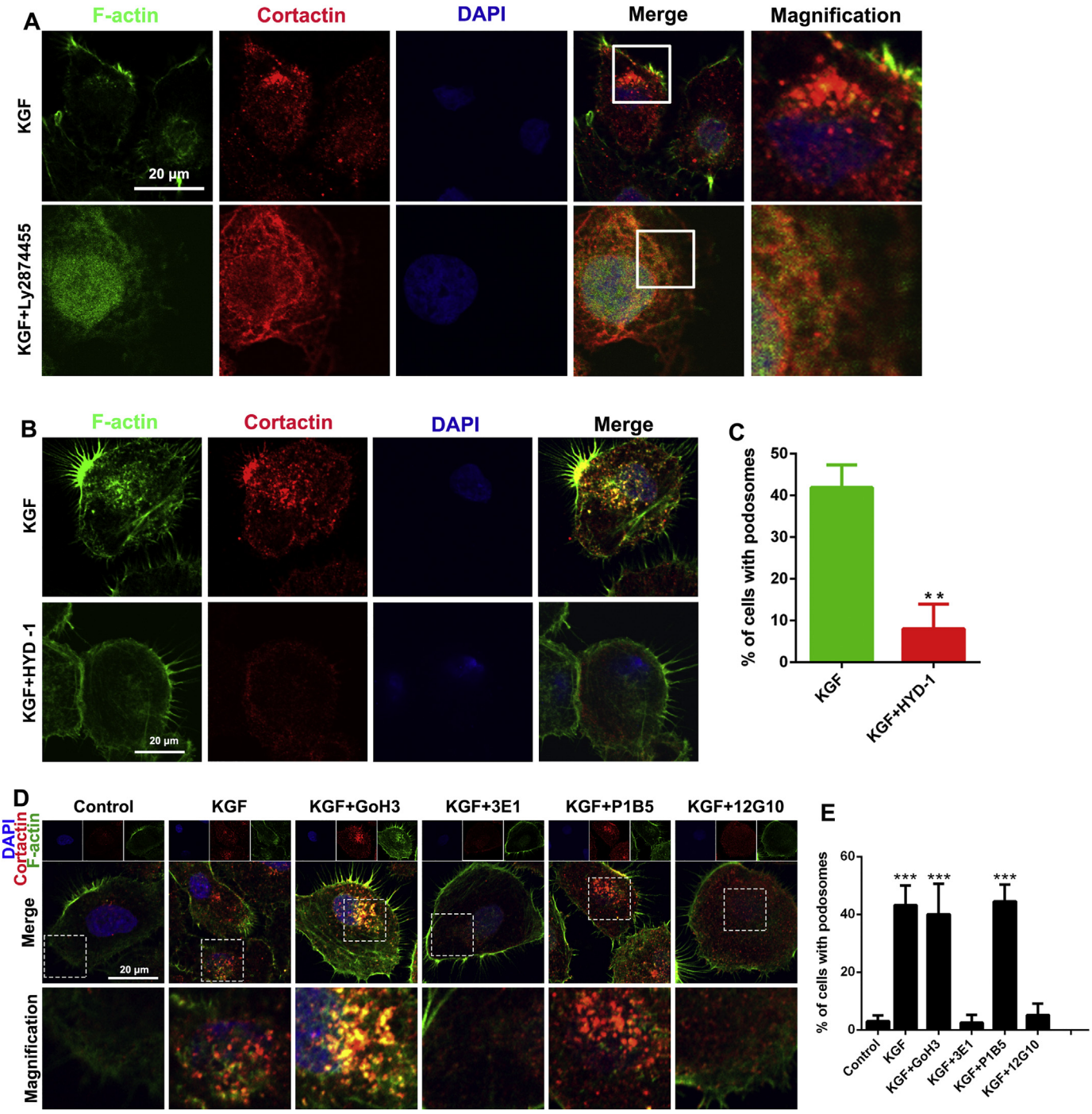

Fig. 3. Integrins are involved in KGF-induced podosome formation. (A) Pretreatment of KGFR inhibitor Ly2874455 15 min before KGF stimulation drastically inhibited the formation of podosomes within HIOECs. (B) HYD-1, an antagonist to integrin subunits α6, β4, α3, and β1, significantly inhibited the KGF-induced podosome formation in HIOECs. (C) $n = 3$ independent experiments in which 100 cells per experiment were analyzed. (D) The impact of function-blocking antibodies against integrin subunits α6 (GoH3), β4 (3E1), α3 (P1B5), and β1 (12G10) on the KGF-induced podosome formation in HIOECs. (E) The statistical analysis of percentage of HIOECs with podosomes each group. GoH3, function-blocking antibody against integrin subunit α6. 3E1, function-blocking antibody against integrin subunit β4; P1B5, function-blocking antibody against integrin subunit α3; 12G10, function-blocking antibody against integrin subunit β1. $n = 3$ independent experiments in which 100 cells per experiment were analyzed. Data are expressed as the mean ± SD. $^{**}P < 0.01$. $^{***}P < 0.001$.

integrin associated proteins, such as vinculin and paxillin [16]. Therefore, we further detected the localization of WASP in the core of podosome-like structures, and the localization of vinculin with cortactin in the ring of podosome-like structures. The results demonstrated that these podosome-like structures characteristically contain WASP in the center, which is surrounded by a ring of integrin associated proteins including vinculin (Fig. 1C and D). Next, we investigated the other podosomal components in the podosome-like structures (identified by colocalization of F-actin-cortactin at the ventral side of the cell). The results showed that integrin subunits α6, β4, α3, β1, and MMP14 co-localized with F-actin in podosome-like structures (Fig. 1E-F, data for integrin subunits α3, β1, and MMP14 not shown). To ascertain the ability of the podosome-like structures to degrade matrix, we then performed matrix degradation assays. The results indicated that matrix

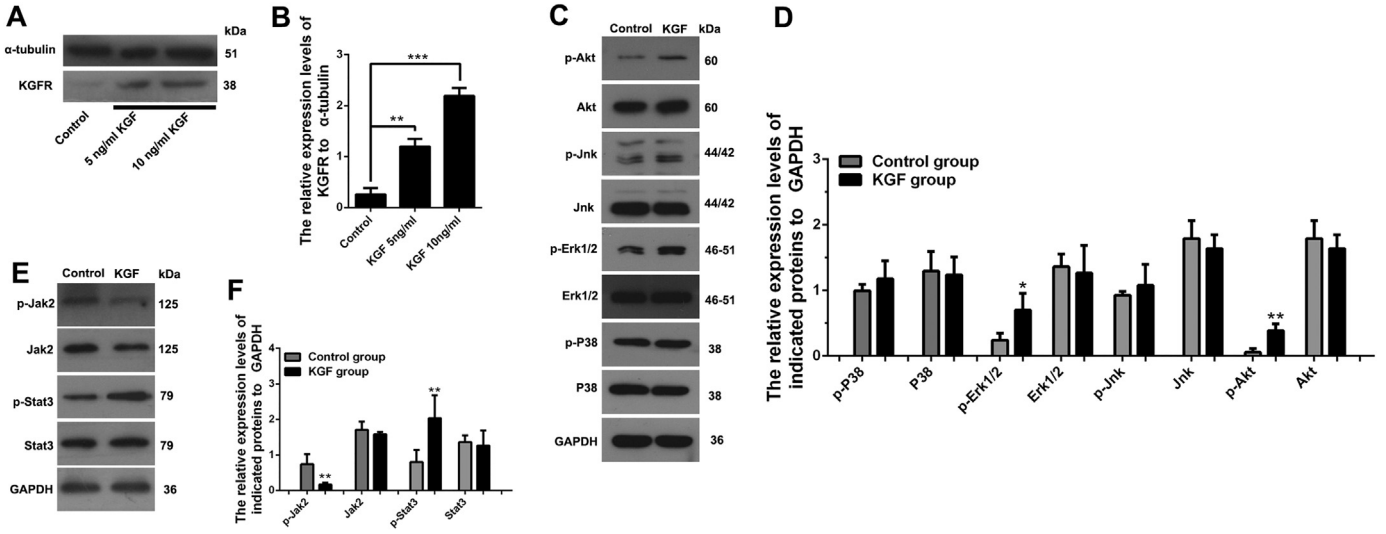

Fig. 4. KGF mediated its effects on HIOECs through Erk1/2 and Akt signaling. Y-axes of Fig. 4B, D, and F referred to the relative expression levels of indicated proteins to the housekeeping gene. (A and B) Western blot detection of the expression level of KGFR in HIOECs after KGF treatment, (C and D) the phosphorylation level of Jak2 and Stat3 after KGF stimulation for 15 min, and (E and F) the phosphorylation level of Erk1/2, p38, Jnk, and Akt after KGF stimulation for 15 min. $n = 3$ independent experiments. Analysis of matrix protein expression in protein extracts from each group by ImageJ. Data are expressed as the mean ± SD. $^{*}P < 0.05$, $^{**}P < 0.01$, $^{***}P < 0.001$.

degradation, which has previously been associated with podosomes, was observed in HIOECs with podosomes (Fig. 2A and B). And to further analyze the possible synergistic effect between cell adhesion and matrix degradation, we detected the colocolization between integrin β1 and MMP14. Our results demonstrated that integrin β1 was colocolized with MMP14 in podosomes within HIOECs (Fig. 2C).

3.2. Integrins are involved in KGF-induced podosome formation

Because KGF mainly exerted its effects on epithelial cells via keratinocyte growth factor (KGFR), we explored the impact of KGFR inhibitor Ly2874455 (Selleck, S7057) on KGF-induced podosome formation in HIOECs. Pretreatment of 10 μM Ly2874455 15 min before KGF stimulation drastically inhibited the formation of podosomes within HIOECs (Fig. 3A). A recent study demonstrated that KGF simultaneously enhanced oral rete peg elongation and epithelial adhesion [11]. However, inhibition of integrins with HYD-1, an antagonist to integrin α6, β4, α3, and β1, drastically abrogated the KGF-induced oral epithelial adhesion and rete peg elongation, indicating the role of integrins in adhesion and matrix remodeling. Because adhesion and matrix degradation are two major podosome functions, we wonder whether integrins are functionally implicated in KGF-induced podosome formation in HIOECs. Therefore, we pretreated HIOECs with HYD-1 to analyze the impact of integrins on KGF-induced podosome formation. As shown in Fig. 3B and C, HYD-1 significantly abrogated the KGF-induced podosome formation. Importantly, HYD-1 can simultaneously inhibit the function of integrin subunits α6, β4, α3, and β1 [17]. To further analyze the relative importance of integrin subunits α6, β4, α3, and β1 in KGF-induced podosome formation, we treated HIOECs with their specific function-blocking antibodies GoH3, 3E1, P1B5, and 12G10 respectively. The results showed that inhibition of integrin subunit β4 with 3E1 and β1 with 12G10 significantly impaired podosome formation, while inhibition of integrin subunit α6 with GoH3 and α3 with P1B5 had only a marginal effect on KGF-induced podosome formation (Fig. 3D and E).

3.3. KGF mediated its effects on HIOECs through Erk1/2 and Akt signaling

In the present study, we detected the phosphorylation level of Erk1/2, p38, Jnk, Akt, Jak2, and Stat3 in HIOECs by Western blot 15 min after KGF treatment. The results showed that the expression level of KGFR and phosphorylation levels of Erk1/2, Akt, and Stat3 were upregulated 10 min after 10 ng/mL KGF treatment, whereas the phosphorylation levels of p38 and Jnk were unaffected (Fig. 4A-F). Notably, the phosphorylation level of Jak2 was significantly downregulated. Jak2 is considered to be the upstream molecule of Stat3, but their phosphorylation levels showed an inverse relationship. These results indicated that KGF mediated its effects on HIOECs possibly through Erk1/2 and Akt signaling.

3.4. Erk1/2 plays an essential role in KGF-induced podosome formation

Although both Erk1/2 and Akt were significantly activated in HIOECs, we wondered whether both Erk1/2 and Akt were indispensable for KGF-induced podosome formation. To explore the impact of Erk1/2 and Akt blockade on KGF-induced podosome formation, we inhibited Erk1/2 using their specific inhibitors U0126, and inhibited Akt using Ly294002 and MK2206. The HIOECs were firstly incubated with 10 μM U0126, Ly294002 and 20 μM MK2206 for 15 min, and then treated with KGF for 24 h. Notably, only inhibition of Erk1/2 abrogated the KGF-induced podosome formation, whereas inhibition of Akt only had marginal effects on podosome formation in HIOECs (Fig. 5A-F). Moreover, statistical analysis indicated that inhibition of Erk1/2 also reduced the average podosome numbers within HIOECs (Fig. 5G).

3.5. Integrins are key mediators between KGF and Erk1/2 activation

As inhibition of integrin subunits β4 and β1 and Erk1/2 abrogated KGF-induced podosome formation, we wondered whether the KGF induced-Erk1/2 activation was associated with integrin subunits β4 and β1. To test this hypothesis, we suppressed the expression of β4 and β1 integrin with specific siRNAs, verifying the efficiency of the siRNAs by Western blot and real-time PCR (data not shown). The results showed that knockdown of integrin subunits β4 and β1 significantly downregulated the phosphorylation level of Erk1/2 and Akt in HIOECs (Fig. 5A-D). We further analyzed the impact of specific inhibitors U0126 (10 μM) and Ly294002 (10 μM) on the expression levels of integrins. The results demonstrated that inhibition of both Erk1/2 and Akt significantly upregulated the expression levels of integrin subunits β4 and β1 (Fig. 5E-H). These data suggested that integrin subunits β4

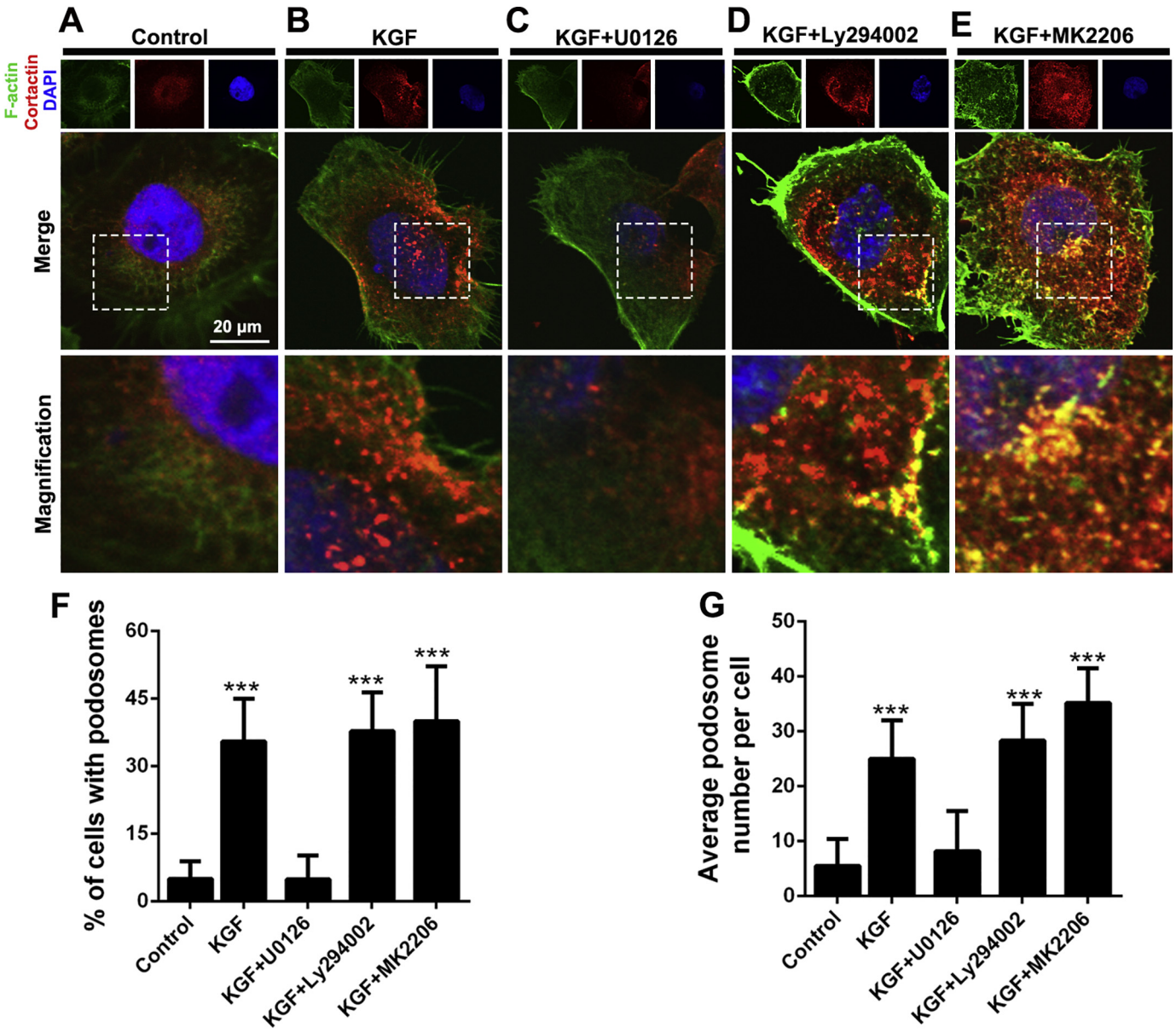

Fig. 5. Impact of Erk1/2 and Akt blockade on KGF-induced podosome formation. U0126, specific inhibitor of Erk1/2; Ly294002 and MK2206, specific inhibitor of Akt. (A, B and E) 24 h after KGF treatment, the ratio of cells containing F-actin-cortactin complexes in the KGF group was significantly elevated compared to the control group. (C and E) U0126 significantly inhibited the KGF-induced podosome formation in HIOECs. (D and E) Ly294002 and MK2206 had a marginal effect on KGF-induced podosome formation in HIOECs. n = 3 independent experiments in which 100 cells per experiments were analyzed. Data are expressed as the mean ± SD. ***$P < 0.001$.

and β1 were essential mediators between KGF and phosphorylation of Erk1/2 and Akt in HIOECs.

4. Discussion

In the present study, we explored the possibility of podosome formation in HIOECs after KGF treatment. The results demonstrated that the podosome-like structures in HIOECs presented as dot-like structures with a diameter of 0.4 μm, which were similar in shape to those found in osteoclasts [18]. Moreover, the key components of podosomes including integrins and MMP14 closely surrounded the F-Actin-cortactin core, suggesting the adhesion and matrix degradation functions of the podosome-like structures. Most importantly, the podosome-like structures in HIOECs indeed had the ability to degrade matrix. Based on these results, we consider that KGF can promote the formation of podosomes in HIOECs, which may be a reasonable mechanism underlying dynamic adhesion during oral mucosal rete peg elongation.

In addition to growth factors and cytokines, integrins, one of the key components of podosomes, also play essential roles in the assembly and function of podosomes in various cell types. For example, β2 integrin participates in podosome formation in dendritic cells, whereas β3 integrin contributes to podosome formation in osteoclasts [19]. A recent study demonstrates that α6β1 integrin is essential for VEGF-induced endothelial podosome rosettes [8]. The integrin subunits of α6, β4, α3, and β1 are the dominant types expressed in keratinocytes [20]. In the present study, we found that the number of podosomes was significantly reduced upon inhibition of the function of integrin subunits β1 and β4 with their specific function-blocking monoclonal antibodies, indicating the role of integrin subunits β4 and β1 in podosome assembly in HIOECs. Many studies have demonstrated that integrins also play important roles in podosome self-renewal. For example, Gawden-Bone et al. found that mutation in amino acids 745 or 746 in integrin β2

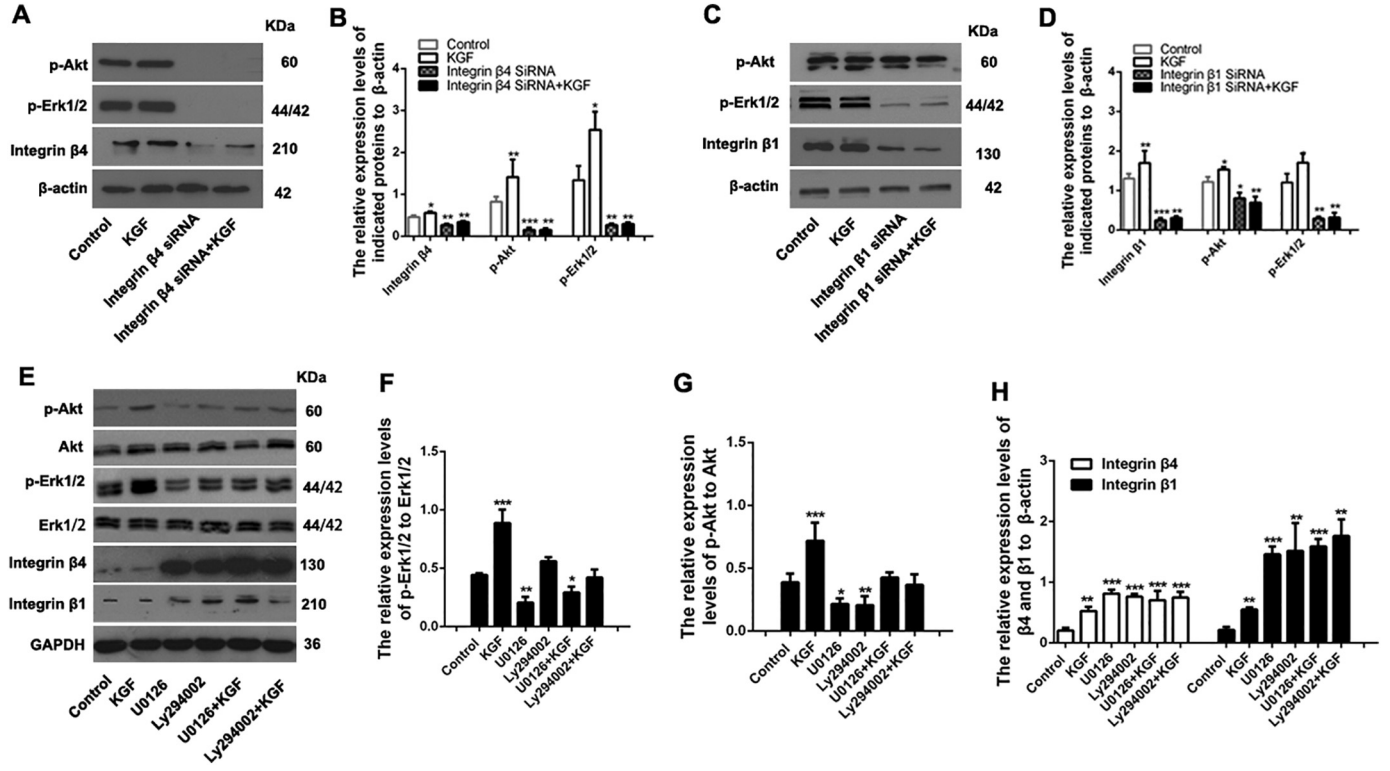

Fig. 6. Integrins are key mediators between KGF and activation of Erk1/2. Y-axes of Fig. 6B, D, F, G, and H referred to the relative expression levels of indicated proteins to the housekeeping gene. (A and B) Knockdown of integrin β4 by specific siRNA significantly inhibited the expression level of integrin β4 and downregulated the phosphorylation levels of Erk1/2 and Akt. (C and D) Knockdown of integrin β1 by specific siRNA significantly inhibited the expression level of integrin β1 and downregulated the phosphorylation levels of Erk1/2 and Akt. (*E*-G) U0126 and Ly294002 significantly downregulated the phosphorylation levels of Erk1/2 and Akt. (E and H) U0126 and Ly294002 significantly inhibited the expression levels of integrin subunits β4 and β1. n = 3 independent experiments. Data are expressed as the mean ± SD. $^{*}P < 0.05$, $^{**}P < 0.01$, $^{***}P < 0.001$.

inhibited the disassembly of podosomes mediated via Toll-like receptors [19]. Therefore, we hypothesize that integrin subunits β4 and β1 may have a role in different stages of podosome formation and renewal. Notably, these integrin-specific, function-blocking monoclonal antibodies could block adhesion of cells to the ECM (i.e., laminin, or collagen). Meanwhile, loss of adhesion from the receptors might impair the outside-in signaling mediated by integrins. Therefore, although we inferred that these function blocking antibody inhibited the interaction between HIOECs and matrix, whether these function-blocking antibodies blocked the outside-in signaling warranted further investigation.

Inhibition of integrins significantly downregulated the KGF-induced phosphorylation of Erk1/2 and Akt, whereas inhibition of Erk1/2 and Akt significantly upregulated the expression of integrin α6, β4, α3, and β1. Therefore, integrins are key mediators between KGF and activation of Erk1/2 and Akt in HIOECs, which is reminiscent of previously described crosstalk between growth factors and integrins [21]. Integrin ligation has been demonstrated to induce a series of intracellular signaling pathways including MAPK, FAK, Src, small GTPases, and PI3K. Interestingly, these signaling effectors are also activated after growth factor stimulation. Furthermore, integrins can directly associate with growth factor receptors. For example, integrin αvβ3 is directly linked with PDGFR and VEGFR in endothelial cells [22]. More importantly, some growth factors such as IGF interact directly with integrins [23]. Therefore, the crosstalk between integrins and growth factors and/or growth factor receptors can propagate downstream signaling by regulating the capacity of integrin/growth factor receptor complexes. Presumably, Erk1/2 and Akt may be one of the points of crosstalk between KGF and integrins; however, the concrete mechanisms warrant further investigation.

Our results demonstrated that only Erk1/2 and not Akt plays an indispensable role in KGF-induced podosome formation, which is in accordance with Gu's study [24]. However, Akt has also been reported to contribute to the assembly of podosomes in multiple cell types including osteoclasts and endothelial cells [25–27]. Various reasons can explain the diversity of regulatory mechanisms for podosome formation. 1) Both adhesion signaling and growth factors can induce podosome assembly [28]. For example, adhesion signaling is crucial for podosome organization and maturation in osteoclasts, whereas a multiplicity of growth factors including PDGF, VEGF, and TGF-β induce the assembly of podosomes in nonmyeloid cells, such as endothelial cells and smooth muscle cells [29]. 2) Although podosomes in various cell types show parallel functions in promoting adhesion and matrix remodeling, their morphologies are different [9]. For example, in v-Src-transformed NIH 3 T3 fibroblasts, podosomes present as rosette-like structures (Seals et al. 2005), whereas phorbol ester-induced podosomes in human airway epithelial cells present as numerous small dots with occasional rosette rings and belts (Xiao et al. 2009). 3) Multiple integrins including integrin subunits β2, β3, α6β1 are involved in the assembly, maturation, and renewal of podosomes in several cell types [4]. Therefore, the downstream signaling pathways mediating these upstream inputs are varied. Notably, downstream signaling pathways involved in podosome assembly always converge on common signaling hubs, especially Rho family GTPases including Rac/Cdc42 and p21-activated kinase (Pak), which ultimately control podosome formation and maturation via regulating cytoskeleton rearrangement [28,30,31].

Current views suggest podosomes are special F-actin-rich matrix-degrading structures found in both normal and pathologic cells. For example, the special role of F-actin and MMP within invadopodia in ECM degradation during oral squamous cell carcinoma formation and invasion has been demonstrated [32]. In addition, De Vicente et al. found that cortactin overexpression was a significant predictor of increased cancer risk in oral mucosal premalignant lesions [33].

Therefore, these findings not only have relevance to importance of oral epithelial functions, but may also contribute to the related study focusing on the pathogenesis of oral mucosal diseases such as oral squamous cell carcinoma.

5. Conclusion

In summary, this work identified podosome assembly in HIOECs after KGF treatment, during which integrin-Erk1/2 signaling plays an indispensable role. The availability of integrins and MMPs within podosomes facilitates the dynamic adhesion and ECM remodeling ability of HIOECs, indicating the possible role both in oral epithelial functions and pathogenesis of oral diseases.

Acknowledgments

We thank the State Key Laboratory Breeding Base of Basic Science of Stomatology (Hubei-MOST) & Key Laboratory of Oral Biomedicine Ministry of Education, School & Hospital of Stomatology, Wuhan University, particularly Dong Chen, for providing equipment and technical assistance for confocal microscopy experiments.

Competing interests

No competing interests declared.

Author contributions

Guoliang Sa contributed to experiment conception and design; data acquisition, analysis, and interpretation; and drafted the manuscript. Zhikang Liu, Jiangang Ren, Qilong Wan, Xuepeng Xiong, Zili Yu, and Heng Chen contributed to data analysis and interpretation; and critically revised the manuscript. Yifang Zhao and Sangang He contributed to experiment conception, and critically revised the manuscript. All authors declare no potential conflicts of interest for all aspects of the work.

Funding

This research was supported by the National Natural Science Foundation of China grant NO. 81371126 to S.G. He, grant NO. 81600385 to J.G. Ren, and grant NO. 81801842 to Z.L. Yu. The authors declare no potential conflicts of interest with respect to the authorship and/or publication of this article.

References

[1] K.T. Lawlor, P. Kaur, Dermal contributions to human Interfollicular epidermal architecture and self-renewal, Int. J. Mol. Sci. 16 (2015) 28098–28107.
[2] T.F. Wu, X.P. Xiong, W.F. Zhang, H.X. Zou, H.Y. Xie, S.G. He, Morphogenesis of rete ridges in human oral mucosa: a pioneering morphological and immunohistochemical study, Cells Tissues Organs 197 (2013) 239–248.
[3] A.L. Clement, T.J. Moutinho Jr., G.D. Pins, Micropatterned dermal-epidermal regeneration matrices create functional niches that enhance epidermal morphogenesis, Acta Biomater. 9 (2013) 9474–9484.
[4] D.A. Murphy, S.A. Courtneidge, The 'ins' and 'outs' of podosomes and invadopodia: characteristics, formation and function, Nat. Rev. Mol. Cell Biol. 12 (2011) 413–426.
[5] H. Schachtner, S.D. Calaminus, S.G. Thomas, L.M. Machesky, Podosomes in adhesion, migration, mechanosensing and matrix remodeling, Cytoskeleton 70 (2013) 572–589.
[6] T. Daubon, P. Spuul, F. Alonso, I. Fremaux, E. Genot, VEGF-A stimulates podosome-mediated collagen-IV proteolysis in microvascular endothelial cells, J. Cell Sci. 129 (2016) 2586–2598.
[7] C. Varon, F. Tatin, V. Moreau, E. Van Obberghen-Schilling, S. Fernandez-Sauze, E. Reuzeau, I. Kramer, E. Genot, Transforming growth factor beta induces rosettes of podosomes in primary aortic endothelial cells, Mol. Cell. Biol. 26 (2006) 3582–3594.
[8] G. Seano, G. Chiaverina, P.A. Gagliardi, L. di Blasio, A. Puliafito, C. Bouvard, R. Sessa, G. Tarone, L. Sorokin, D. Helley, R.K. Jain, G. Serini, F. Bussolino, L. Primo, Endothelial podosome rosettes regulate vascular branching in tumour angiogenesis, Nat. Cell Biol. 16 (2014) 931–941.
[9] H. Xiao, R. Eves, C. Yeh, W. Kan, F. Xu, A.S. Mak, M. Liu, Phorbol ester-induced podosomes in normal human bronchial epithelial cells, J. Cell. Physiol. 218 (2009) 366–375.
[10] L. Spinardi, J. Rietdorf, L. Nitsch, M. Bono, C. Tacchetti, M. Way, P.C. Marchisio, A dynamic podosome-like structure of epithelial cells, Exp. Cell Res. 295 (2004) 360–374.
[11] G.L. Sa, X.P. Xiong, J.G. Ren, J.Y. Wang, H.F. Xia, Z.K. Liu, S.G. He, Y.F. Zhao, KGF enhances oral epithelial adhesion and rete peg elongation via Integrins, J. Dent. Res. 96 (2017) 1546–1554.
[12] Q. Liang, R.R. Mohan, L. Chen, S.E. Wilson, Signaling by HGF and KGF in corneal epithelial cells: Ras/MAP kinase and Jak-STAT pathways, Invest. Ophthalmol. Vis. Sci. 39 (1998) 1329–1338.
[13] T. Bai, F. Liu, F. Zou, G. Zhao, Y. Jiang, L. Liu, J. Shi, D. Hao, Q. Zhang, T. Zheng, Y. Zhang, M. Liu, S. Li, L. Qi, J.Y. Liu, Epidermal growth factor induces proliferation of hair follicle-derived Mesenchymal stem cells through epidermal growth factor receptor-mediated activation of ERK and AKT Signaling pathways associated with upregulation of cyclin D1 and downregulation of p16, Stem Cells Dev. 26 (2017) 113–122.
[14] S. Braun, M. Krampert, E. Bodo, A. Kumin, C. Born-Berclaz, R. Paus, S. Werner, Keratinocyte growth factor protects epidermis and hair follicles from cell death induced by UV irradiation, chemotherapeutic or cytotoxic agents, J. Cell Sci. 119 (2006) 4841–4849.
[15] W. Xiao, Z.X. Bao, C.Y. Zhang, X.Y. Zhang, L.J. Shi, Z.T. Zhou, W.W. Jiang, Upregulation of miR-31* is negatively associated with recurrent/newly formed oral leukoplakia, PLoS One 7 (2012) e38648.
[16] Y. He, Y. Ren, B. Wu, B. Decourt, A.C. Lee, A. Taylor, D.M. Suter, Src and cortactin promote lamellipodia protrusion and filopodia formation and stability in growth cones, Mol. Biol. Cell 26 (2015) 3229–3244.
[17] I.B. DeRoock, M.E. Pennington, T.C. Sroka, K.S. Lam, G.T. Bowden, E.L. Bair, A.E. Cress, Synthetic peptides inhibit adhesion of human tumor cells to extracellular matrix proteins, Cancer Res. 61 (2001) 3308–3313.
[18] S. Linder, The matrix corroded: podosomes and invadopodia in extracellular matrix degradation, Trends Cell Biol. 17 (2007) 107–117.
[19] C. Gawden-Bone, M.A. West, V.L. Morrison, A.J. Edgar, S.J. McMillan, B.D. Dill, M. Trost, A. Prescott, S.C. Fagerholm, C. Watts, A crucial role for beta2 integrins in podosome formation, dynamics and toll-like-receptor-signaled disassembly in dendritic cells, J. Cell Sci. 127 (2014) 4213–4224.
[20] C. Margadant, R.A. Charafeddine, A. Sonnenberg, Unique and redundant functions of integrins in the epidermis, FASEB J. 24 (2010) 4133–4152.
[21] B.P. Eliceiri, Integrin and growth factor receptor crosstalk, Circ. Res. 89 (2001) 1104–1110.
[22] E. Borges, Y. Jan, E. Ruoslahti, Platelet-derived growth factor receptor beta and vascular endothelial growth factor receptor 2 bind to the beta 3 integrin through its extracellular domain, J. Biol. Chem. 275 (2000) 39867–39873.
[23] Y. Takada, Y.K. Takada, M. Fujita, Crosstalk between insulin-like growth factor (IGF) receptor and integrins through direct integrin binding to IGF1, Cytokine Growth Factor Rev. 34 (2017) 67–72.
[24] Z. Gu, J. Kordowska, G.L. Williams, C.L. Wang, C.M. Hai, Erk1/2 MAPK and caldesmon differentially regulate podosome dynamics in A7r5 vascular smooth muscle cells, Exp. Cell Res. 313 (5) (2007) 849–866.
[25] T. Fey, K.M. Schubert, H. Schneider, E. Fein, E. Kleinert, U. Pohl, A. Dendorfer, Impaired endothelial shear stress induces podosome assembly via VEGF up-regulation, FASEB J. 30 (2016) 2755–2766.
[26] M.L. Kung, H.E. Tsai, T.H. Hu, H.M. Kuo, L.F. Liu, S.C. Chen, P.R. Lin, Y.L. Ma, E.M. Wang, G.S. Liu, J.K. Liu, M.H. Tai, Hepatoma-derived growth factor stimulates podosome rosettes formation in NIH/3T3 cells through the activation of phosphatidylinositol 3-kinase/Akt pathway, Biochem. Biophys. Res. Commun. 425 (2012) 169–176.
[27] M. Shinohara, M. Nakamura, H. Masuda, J. Hirose, Y. Kadono, M. Iwasawa, Y. Nagase, K. Ueki, T. Kadowaki, T. Sasaki, S. Kato, H. Nakamura, S. Tanaka, H. Takayanagi, Class IA phosphatidylinositol 3-kinase regulates osteoclastic bone resorption through protein kinase B-mediated vesicle transport, J. Bone Miner. Res. 27 (2012) 2464–2475.
[28] D. Hoshino, K.M. Branch, A.M. Weaver, Signaling inputs to invadopodia and podosomes, J. Cell Sci. 126 (2013) 2979–2989.
[29] M. Quintavalle, L. Elia, G. Condorelli, S.A. Courtneidge, MicroRNA control of podosome formation in vascular smooth muscle cells in vivo and in vitro, J. Cell Biol. 189 (2010) 13–22.
[30] C. Albiges-Rizo, O. Destaing, B. Fourcade, E. Planus, M.R. Block, Actin machinery and mechanosensitivity in invadopodia, podosomes and focal adhesions, J. Cell Sci. 122 (2009) 3037–3049.
[31] S. Linder, M. Aepfelbacher, Podosomes: adhesion hot-spots of invasive cells, Trends Cell Biol. 13 (7) (2003) 376–385.
[32] H.M. Li, J.G. Yang, Z.J. Liu, W.M. Wang, Z.L. Yu, J.G. Ren, G. Chen, W. Zhang, J. Jia, Blockage of glycolysis by targeting PFKFB3 suppresses tumor growth and metastasis in head and neck squamous cell carcinoma, J. Exp. Clin. Cancer Res. 36 (2017) 7.
[33] J.C. de Vicente, P. Rosado, P. Lequerica-Fernandez, E. Allonca, L. Villallain, G. Hernandez-Vallejo, Focal adhesion kinase overexpression: correlation with lymph node metastasis and shorter survival in oral squamous cell carcinoma, Head Neck 35 (2013) 826–830.